UCID--21832

DE90 010204

Thermal and Stress Analysis of Hot Isostatically Pressed, Alumina Ceramic, Nuclear Waste Containers

Yun Chang and Clarence L. Hoenig

Manuscript date: March 1, 1990

List of Figures

Contents

Thermal and Stress Analysis of Hot Isostatically Pressed, Alumina Ceramic, Nuclear Waste Containers

Introduction

The Yucca Mountain Project is studying design and fabrication options for a safe durable container in which to store nuclear waste underground at Yucca Mountain, Nevada. The ceramic container discussed here is an alternative to using a metal container. This ceramic alternative would be selected if site conditions prove too corrosive to use metals for nuclear waste storage.

One container concept shown in Fig. 1 has two high-density aluminum oxide (Al_2O_3) sections that were prefabricated by hot isostatic pressing (HIP). After inserting the spent fuel container, the container assembly would be sealed or closed at the joint between the alumina sections. HIP could also be used in the closure process to apply a maximum local pressure to the sealing surface. High pressures available by HIP may be needed to provide a reliable seal at modest temperatures. In this HIP process, the closure material is placed between the two alumina sealing surfaces, then the outer steel jacket is welded to hermetically seal the container, and finally the assembled container is closed by HIP.

Some of the engineering problems addressed in this study were:

- *The stress generated in the alumina container by compressive loads when 4000 to 40,000 psi of external pressure is applied.* Although the minimum compressive stress has not been determined for bonding at the Al_2O_3 interface, we assumed a maximum external pressure of 40,000 psi in this analysis (Note: only 30,000 psi is currently available from commercially produced HIPs).

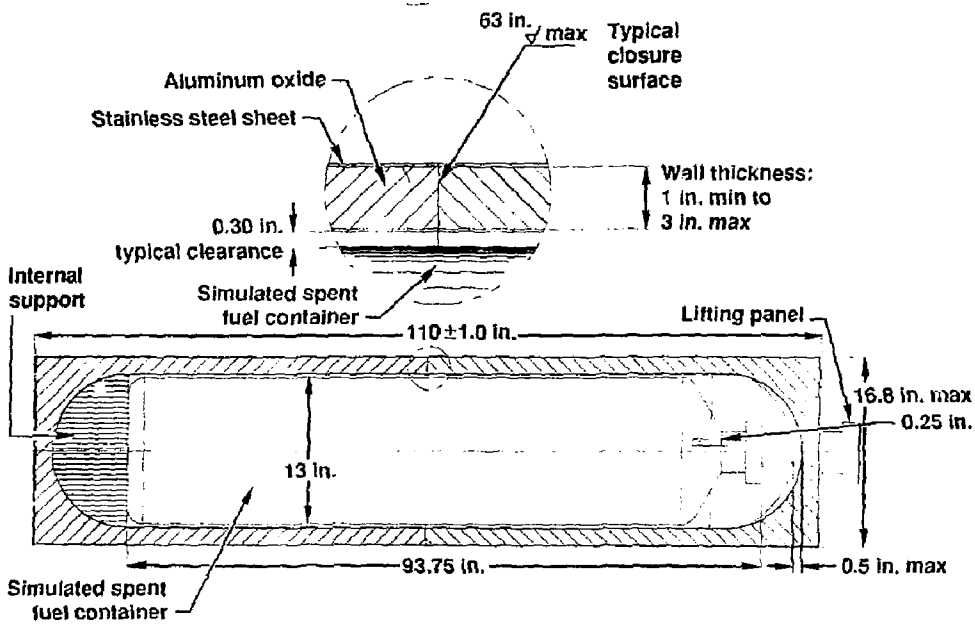

Figure 1. Conceptual design: hot isostatically pressed, alumina ceramic, subscale nuclear waste container.

- *The thermal stress in the container during the heating and cooling processes.* We studied the possibility of using localized heating only in the sealing region. The colder extremities of the container would remain at or near ambient temperature. We also considered the effects of the internal heat output of the simulated spent fuel element package.
- *The temperature histories of the container in various production scenarios and the power required for typical heaters.*
- *The fastest possible turnaround time to heat, seal, and cool the container commensurate with preserving the structural integrity of the ceramic and the closure.* Although several closure materials are now being studied, we confined this evaluation to the alumina container.
- *The testing of some commercial heating elements to determine the maximum available heat output.*
- *The trade-offs between the minimization in thermal stress and cycle time for closure.*

Analysis

The analyses were performed on an engineering prototype of the ceramic container. It was a half-scale model with 110-in. length, 16.8-in. o.d., and a variable alumina wall thickness (Fig. 1). External pressure was applied in 4000psi increments up to 40,000 psi. We then compared the stresses for three wall thickness (1, 2, and 3 in.) under the same external pressure.

The thermal histories were studied with a typical spent-fuel-element package in place. In this experimental setup:

- Spent fuel bundles stored inside the container would release 2210 to 3420 W, depending on the packing configuration.[1] Based on the maximum heat that the fuel bundles could release, we calculated the average heat density (0.24 W/in.^{2}) applied to the container's internal surface.
- No forced convective cooling was planned for the container during the HIP closure process. We assumed a natural convection to 22°C ambient temperature.
- Heat loads from the heater were applied to the container for two different cases:
  1. Constant temperature boundaries were defined locally at the joining area, the container, and the end cap. A steady-state temperature gradient over the entire container was then established between these two temperature boundaries. Heat load to the container in this case was a constant.
  2. Two radiant heaters (7.58 and 11.37 W/in.^{2}) with profiled surface temperatures were applied. Under these conditions, the heat load to the container is a function of temperature difference between the heater and the heated area of the container. Furthermore, the heater temperature can be controlled and profiled by the input power. For each case, temperature histories and thermal stresses were calculated.

We used the TOPAZ2D and NIKE2D computer codes to carry out these calculations.

Material Properties and Operating Conditions

Commercially available alumina (Al_2O_3) was used in this container study. This material, typical of most ceramics, has very high compressive strength, which is favorable to this application. (For example: Coors AD-85 alumina ceramic has a compressive strength at room temperature of 280,000 psi. For AD-90, it is 360,000 psi). The following is a list of the mechanical and thermal properties published by the Coors Ceramics Company that were used in these analyses. (The properties and effects of the metal jacket were not considered in this preliminary study.)

Modulus of elasticity	55.0×10^6 psi
Shear modulus	18.0×10^6 psi
Poisson's ratio	0.21
Tensile strength (1000°C)	14,000 psi
CTE	
(25°C)	3.4×10^{-6}°C
(500°C)	6.0×10^{-6}°C
(1000°C)	8.0×10^{-6}°C
Thermal conductivity (400°C)	0.24 g·cal/s/cm/°C
Specific heat	0.21 g·cal/g/°C
T_{max}	850°C for closure
P_{max}	40,000 psi

Results

Stress vs Wall Thickness and Pressure at Room Temperature

The stresses of three different wall thicknesses (1, 2, and 3 in.) under compression at room temperature were compared under the same range of external pressures. These studies showed that the dominate stress in the container is compressive. In some cases, however, low-level tensile stresses were developed. The ceramic is strong in compression; therefore, for stress considerations alone, a 2- to 3-in.-thick wall would be adequate for the container.

The major stresses were calculated for a maximum 40,000-psi external pressure (Fig. 2). The axial stress component is parallel to the longitudinal axis of the container. The hoop stress is along the circumference of the container. The radial stress is radial from the center of the container. These stresses are listed in Table 1.

In Fig. 3, we show a container with a 1-in.-thick wall to amplify and delineate the deformation effects under compression. (Only a quadrant of the container was modeled because of symmetry.) Nodes marked in this figure indicate the locations in the container where stresses were plotted.

We show the 1-in. wall thickness in Fig. 3 to demonstrate the locations of extreme stress. In reality, we do not expect to use a 1-in. wall thickness. From the standpoint of practical ceramic fabrication, we believe a 2- to 3-in.-thick wall will be more acceptable.

Table 1. Major stresses calculated for a maximum 40,000-psi external pressure.

	At 40,000-psi external pressure		
Wall thickness	Max. radial stress (psi)	Max. axial stress (psi)	Max. hoop stress (psi)
1-in.	1.74×10^5	1.87×10^5	3.25×10^5
2-in.	9.42×10^4	1.07×10^5	1.91×10^5
3-in.	6.85×10^4	8.11×10^4	1.46×10^5

Stress vs Steady State Temperature and Pressure for a 3-in.-thick Wall

Major stress contours and stress plots have been calculated as a function of external pressure and temperature for a wall thickness of 3 in. The boundary conditions were defined assuming an outer surface temperature of 850°C over a region 4 in. from the bonding joint. The end cap temperature at the extremity of the container was taken as 250°C. The temperature gradient was for a steady-state condition. Figures 4 and 5 show the temperature gradients at two locations in the container. In Figs. 6–8, stress contours are shown for the three principle stresses at an 850°C bonding temperature and 20,000-psi pressure. In Fig. 9–11, stresses are plotted as a function of

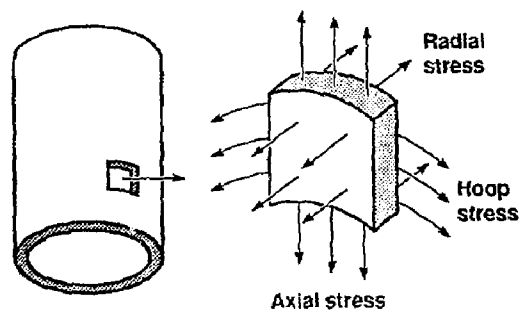

Figure 2. Major stress components.

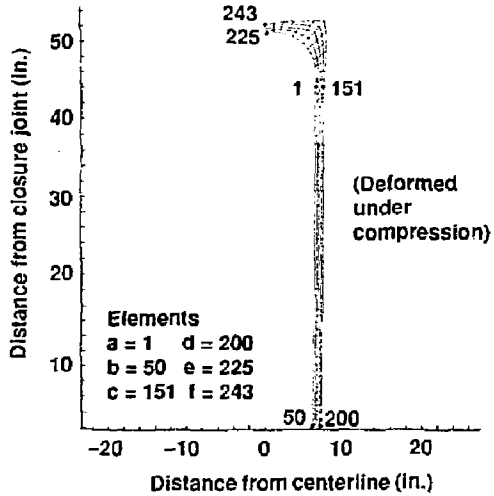

Figure 3. Model in deformed condition (half scale, 1-in.-thick-wall container).

pressure up to 40,000 psi at the six locations of the container shown in Table 2.

In Table 2, major stresses are calculated for various locations as a function of applied external HIP pressures up to 40,000 psi. To compare these stresses at different locations and under different conditions, it will be necessary to represent the three stress components with an approximate single stress value. It is essential to understand that these calculated combined stresses are only intended to show where regions of high stress are located. These stress values should not be used to assess the fracture strength of the material. Depending on the failure theory applicable to the particular ceramic material, other stress values will need to be considered in the final design. For this study, we have used the following equation[2] to calculate the combined stress listed in Table 2.

$$2S^2 = (s1 - s2)^2 + (s2 - s3)^2 + (s3 - s1)^2 \quad . \qquad (1)$$

Here, $s1$, $s2$, and $s3$ represent the three stress components, and S represents the combined stress. Both compressive and tensile stresses are shown. Later we show that the tensile component disappears with the application of external pressure. In Table 2, we show that, when uniform HIP pressures (>20,000 psi) are applied, all thermally induced tensile stress is converted to compression. For example, the external bonding surface at location **E** has an axial tensile stress of 7.7 ksi due to steady temperature gradients. With the application of 20,000-psi HIP pressure, the stress is converted to –30.9-ksi compression.

Temperature and Thermal Stress vs Transient State Heating

The thermal histories of a container (3-in.-thick wall) heated at two different heat fluxes are shown in Figs. 12 and 13. In each case, we assumed, ideally, that the heat was applied directly to the surface at a constant rate. However, when a commercial radiant heater is used as the heat source, the rate of net heat deposited on the cylinder surface will no longer be a constant. Instead, the heat deposited will be a function of surface temperature, temperature of the heater, and other factors (e.g., emissivity and shape governing the heat transfer through radiation). In order to achieve good closure, the entire bonding surface must reach a temperature of 850°C. In Fig. 12 (after 12 hr), the 7.58 W/in.^{2} heater is inadequate. Locations **b** and **d** have only reached temperatures in the range of 600–650°C. Figure 13, however, shows that an 11.37 W/in.^{2} heater is adequate because, after 12 hr, the inside bonding location **b** has reached ~850°C and the outside location **d** has reached ~900°C.

We have also studied three cases in which the rate of heating to 1000°C was varied to provide three different heating profiles (see Fig. 14). We selected a bonding temperature of 850°C rather than 1000°C because we anticipate that 850°C will be the maximum required in closure. The time-temperature histories for each heating profile at the four container locations are shown in Figs. 15–17 for a container with a 3-in.-thick wall. The corresponding high-stress locations for each heating profile after 4 hr are shown in Figs. 18–23.

We can see that heating Profile 1 results in the shortest time to 850°C, but it also causes the most stress. This short time is attractive from the production point of view; however, it is equally important not to damage or crack the container during closure. These preliminary evaluations indicate that a ceramic container under uniform HIP compression would not be vulnerable to tensile stress. This is an important finding since ceramics are strong in compression and weak in tension. However, during closure, transient heating will be required, and our study shows that very high stresses are possible in some localized areas. This requires further study.

Table 2. Major stresses in a ceramic container (half-scale, 3-in.-thick wall) as a function of applied HIP pressure and temperature. (Negative numbers are compressive stress; positive are tensile stress.)

Location	Thermal stress only (ksi)	Thermal and HIP pressure 20,000 psi (ksi)	30,000 psi (ksi)	40,000 psi (ksi)
A				
Radial	-5.2	-39.5	-56.6	-73.8
Axial	0	-18.0	-27.0	-36.0
Hoop	-5.1	-32.0	-47.0	-73.0
Combined	5.2	18.9	26.2	37.4
B				
Radial	7.4	-27.8	-42.0	-63.0
Axial	0	-3.6	-6.2	-8.4
Hoop	7.5	-24.0	-51.0	-63.0
Combined	7.5	22.6	41.0	54.6
C				
Radial	-0.2	-18.0	-26.0	-37.5
Axial	-2.2	-45.7	-67.0	-89.0
Hoop	-0.7	-50.0	-75.3	-100.0
Combined	1.8	30.1	45.7	57.8
D				
Radial	-0.2	-4.4	-3.2	-8.0
Axial	3.0	-33.0	-49.2	-65.0
Hoop	-0.7	-61.2	-91.3	-121.0
Combined	-3.5	49.2	76.3	97.9
E				
Radial	0	-20.4	-30.2	-40.0
Axial	7.7	-30.9	-50.2	-69.5
Hoop	-4.9	-56.5	-88.3	-114.0
Combined	11.0	32.2	51.1	64.5
F				
Radial	0	-1.6	-1.1	-1.5
Axial	-8.8	-47.2	-66.5	-85.9
Hoop	-1.7	-78.3	-116.0	-155.0
Combined	8.1	66.8	99.8	133.2

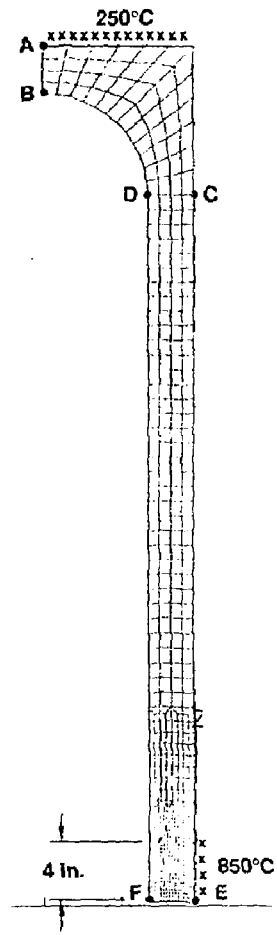

Conclusion and Recommendations

Our preliminary study indicates that the compressive strength of alumina can withstand the application of transient heating and compressive HIP pressures during ceramic closure without cracking or degradation. However, there are preliminary indications of high levels of localized stress during transient heating that must be addressed.

A more complete and expanded analyses should be conducted under the guidelines that follow.

- Analyses should be extended to a full-scale model.
- A follow-up evaluation and optimization of the effects of various heating scenarios on the thermal conditions of enclosed nuclear waste packages should be made.
- More calculations of thermal stresses under transient state conditions should be performed for different closure scenarios.
- Design criteria based on the ceramic failure characteristics of both Al_2O_3 and TiO_2 should be established.

References

1. W. Stein, *Thermal Analysis of NNWSI Conceptual Waste Package Designs*, Lawrence Livermore National Laboratory, Livermore, Calif., UCID-20091 (1984).
2. J. E. Shigley, *Mechanical Engineering Design*, 3rd ed., (McGraw-Hill, New York, NY, 1977).

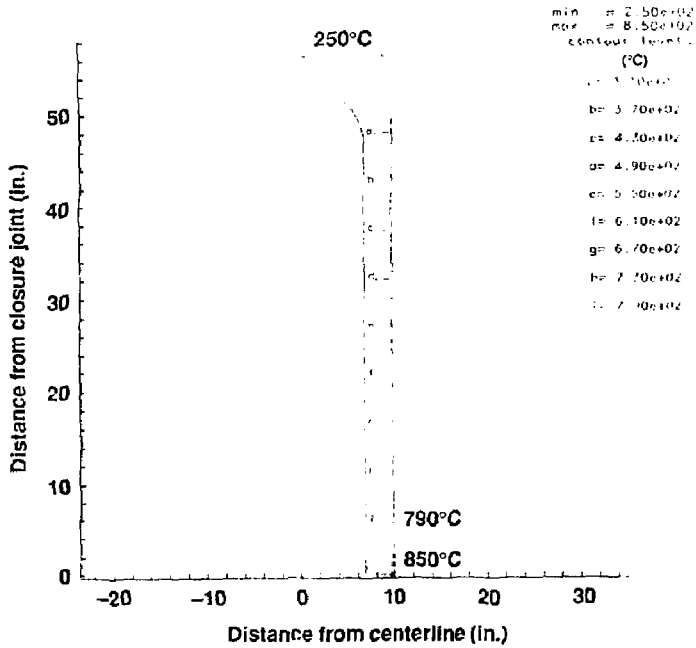

Figure 4. Steady state temperature gradient in an Al_2O_3 container (half scale, 3-in.-thick wall) with a constant surface temperature boundary of 850°C, 4-in. from bonding joint. (Quarter section profile.)

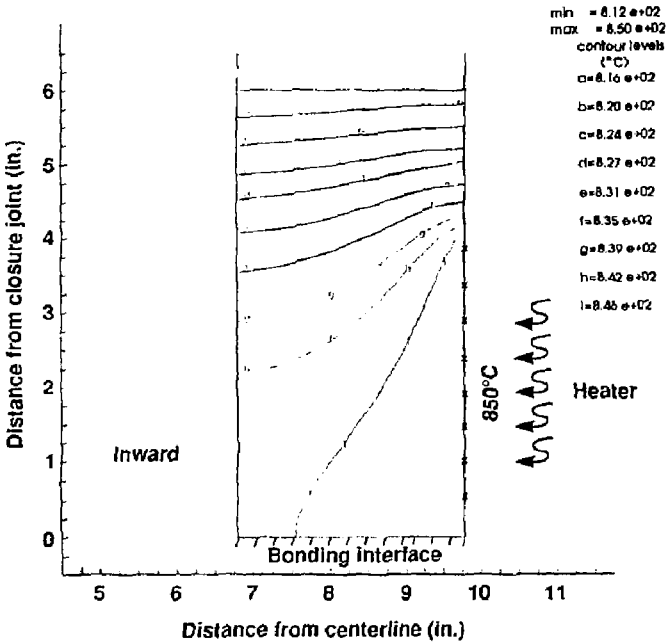

Figure 5. Steady state temperature gradient in an Al_2O_3 container (half scale, 3-in.-thick wall) near the bonding interface. (Localized region at bonding interface.)

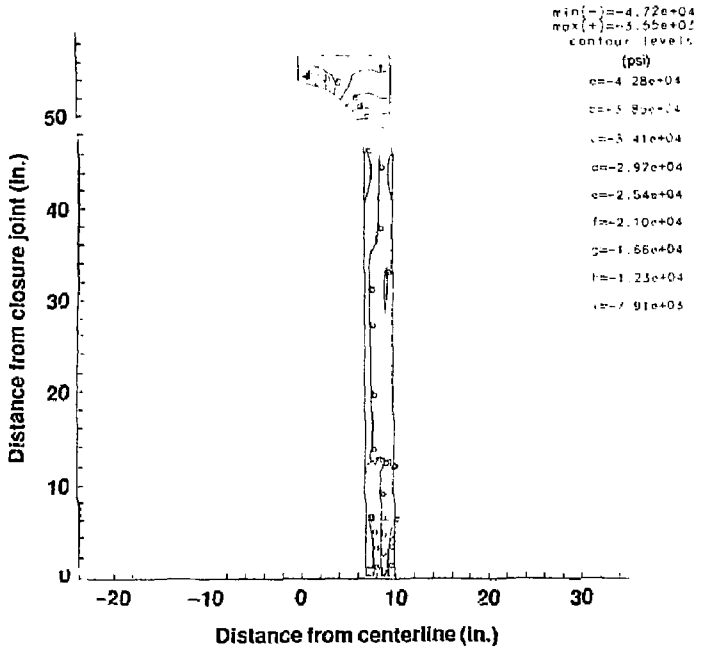

Figure 6. Typical contours of axial stress. Thermal stress in a ceramic vessel (half scale, 3-in.-thick wall) at 850°C localized bonding temperature and 20,000-psi external pressure. (Negative numbers are compressive stress; positive are tensile stress.)

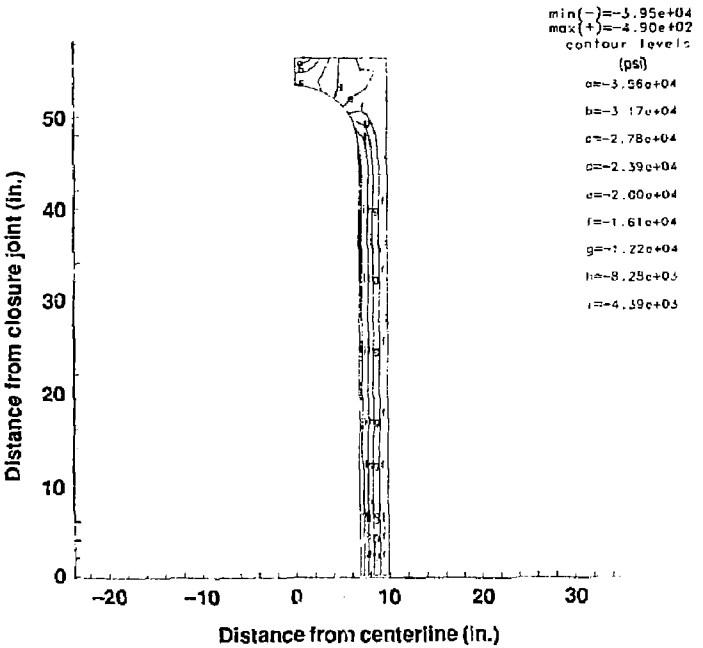

Figure 7. Typical contours of radial stress. Thermal stress in a ceramic vessel (half scale, 3-in.-thick wall) at 850°C localized bonding temperature and 20,000-psi external pressure. (Negative numbers are compressive stress; positive are tensile stress.)

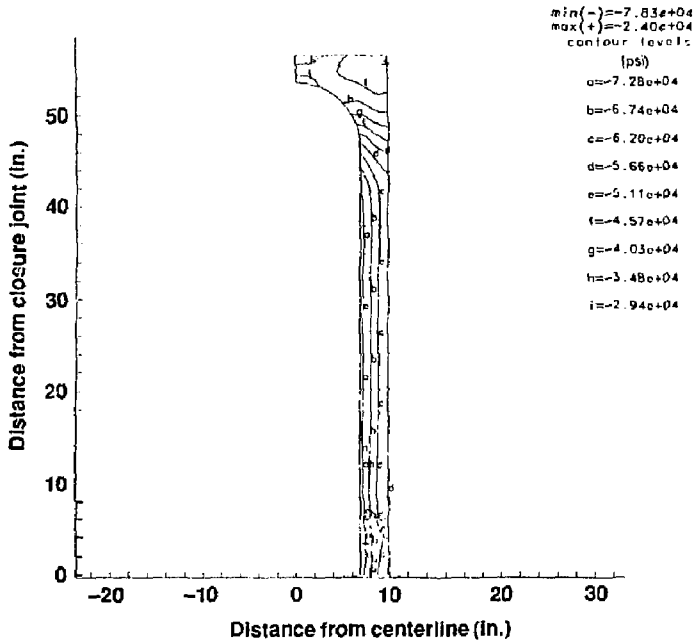

Figure 8. Typical contours of hoop stress. Thermal stress in a ceramic vessel (half scale, 3-in.-thick wall) at 850°C and 20,000-psi external pressure. (Negative numbers are compressive stress; positive are tensile stress.)

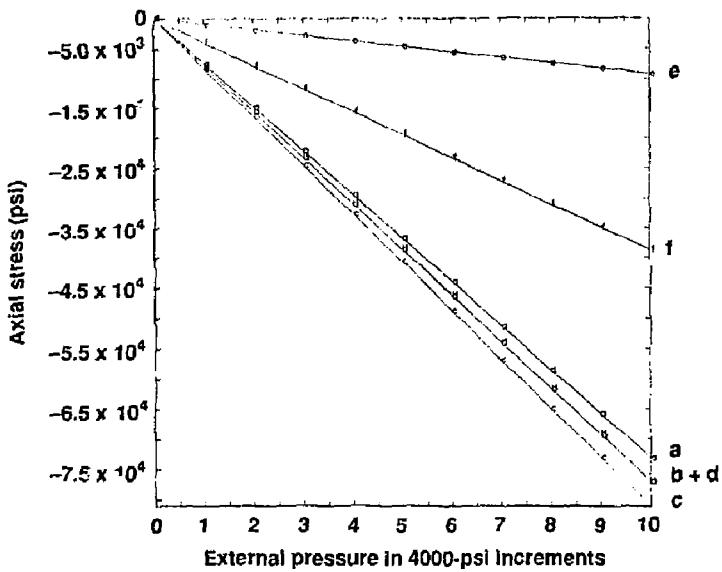

Figure 9. Axial stress in an Al_2O_3 container (half scale, 3-in.-thick wall) under external pressure.

Minimum = –8.1146e + 04
Maximum = 0

Elements
a = 1 c = 151 e = 225
b = 50 d = 200 f = 243

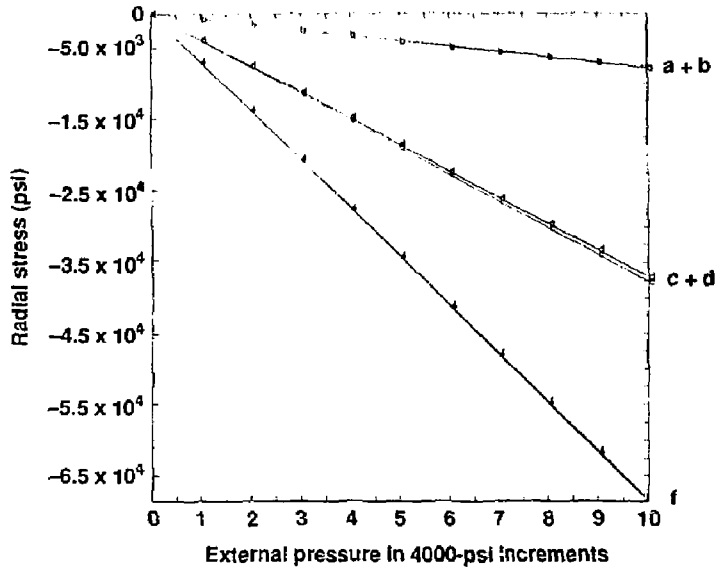

Figure 10. Radial stress in an Al_2O_3 container (half scale, 3-in.-thick wall) under external pressure.

Minimum = −6.8525e + 04
Maximum = 0

Elements
a = 1 c = 151 e = 225
b = 50 d = 200 f = 243

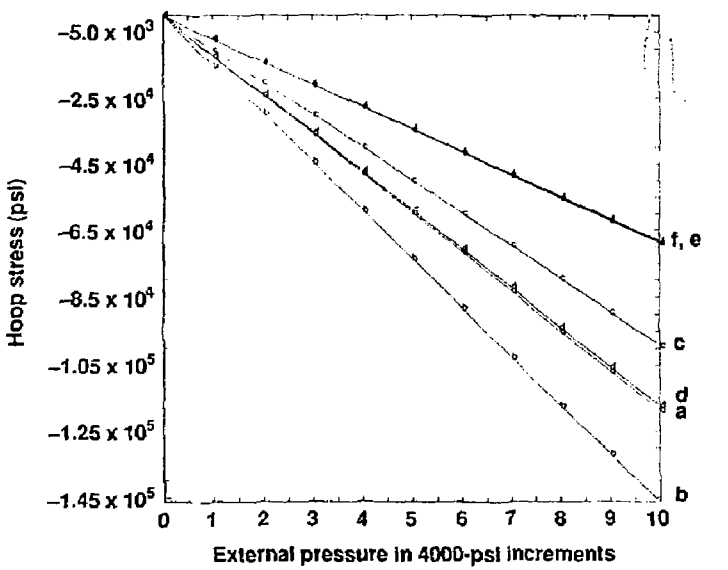

Figure 11. Hoop stress in an Al_2O_3 container (half scale, 3-in.-thick wall) under external pressure.

Minimum = −1.4635e + 05
Maximum = 0

Elements
a = 1 c = 151 e = 225
b = 50 d = 200 f = 243

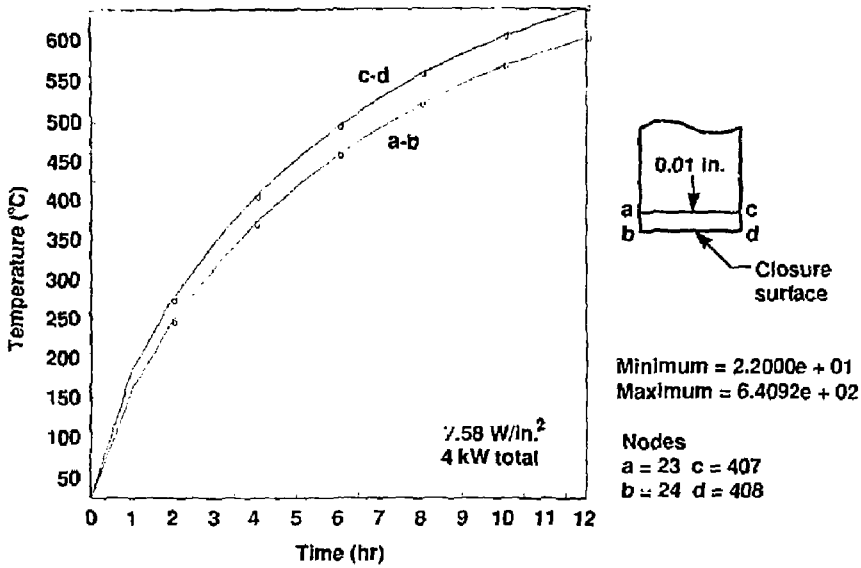

Figure 12. Temperature history of an Al_2O_3 container (half scale, 3-in.-thick wall) with 7.58 W/in.^{2} heater.

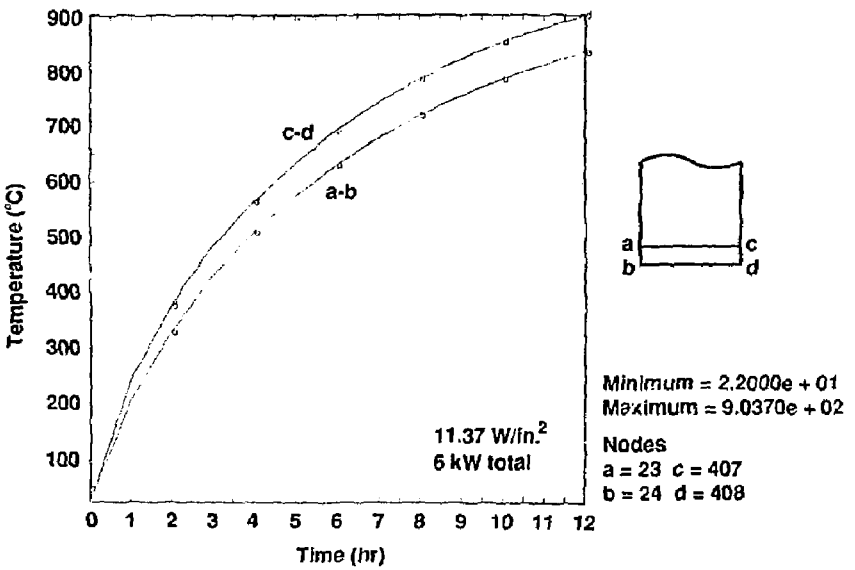

Figure 13. Temperature history of an Al_2O_3 container (half scale, 3-in.-thick wall) with 11.37 W/in.^{2} heater.

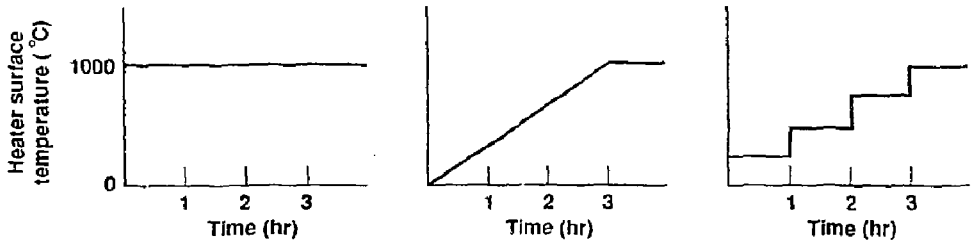

Profile 1: The heater temperature was kept at 1000°C constantly throughout the heating period. This simulates a closure scenario for rapid heating in which a hot clam shell heater (radiant type of heater) is applied directly to a container at or near room temperature.

Profile 2: For more gradual heating, the heater temperature increased steadily from room temperature to 1000°C in 3 hr and then was held at 1000°C throughout the balance of the heating period. This simulates a more modest heat up scenario that will take more time and will reduce thermal shock as a potential problem.

Profile 3: Heating conditions here are comparable to Profile 2. The heater temperature was increased in steps by 250°C every hour to reach 1000°C.

Figure 14. Three heating profiles used to study thermal stress during transient-state heating for an Al_2O_3 container (half scale, 3-in.-thick wall).

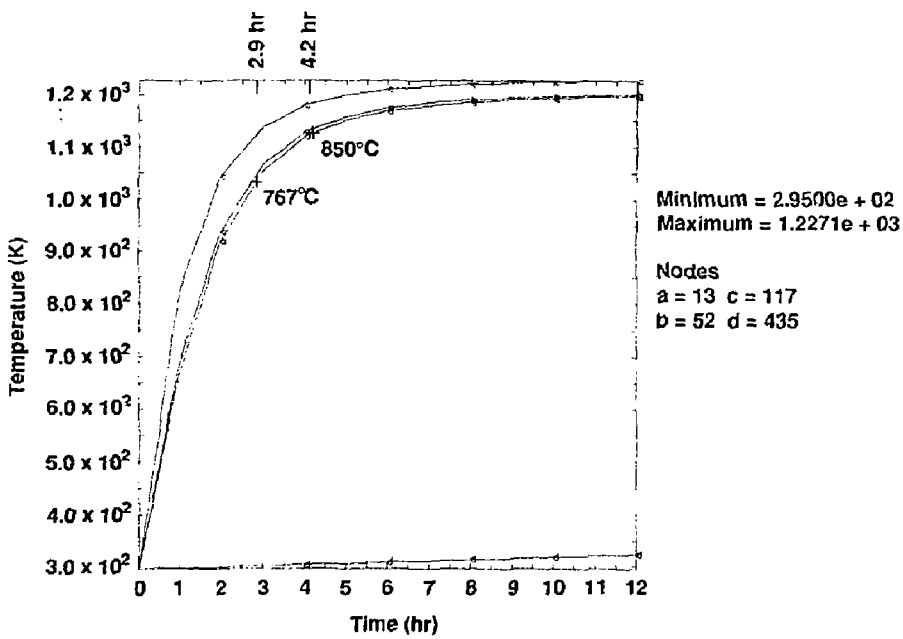

Figure 15. Temperature history of an Al_2O_3 container (half scale, 3-in.-thick wall) with heating Profile 1.

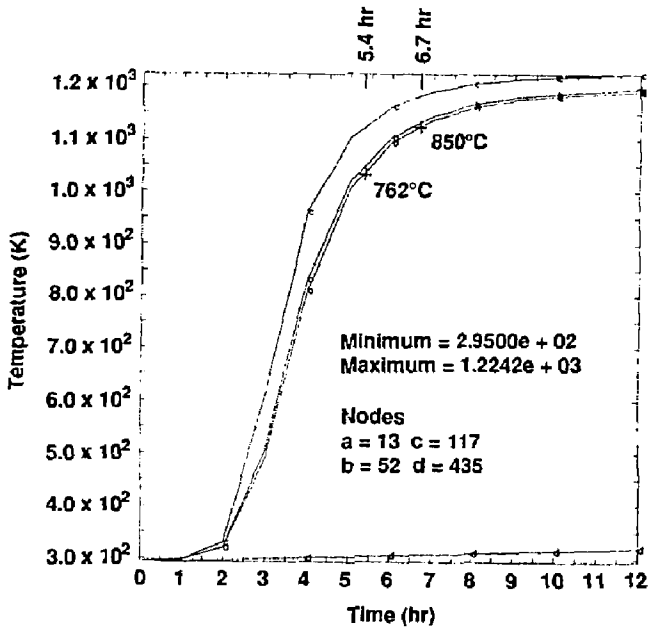

Figure 16. Temperature history of an Al_2O_3 container (half scale, 3-in.-thick wall) with heating Profile 2.

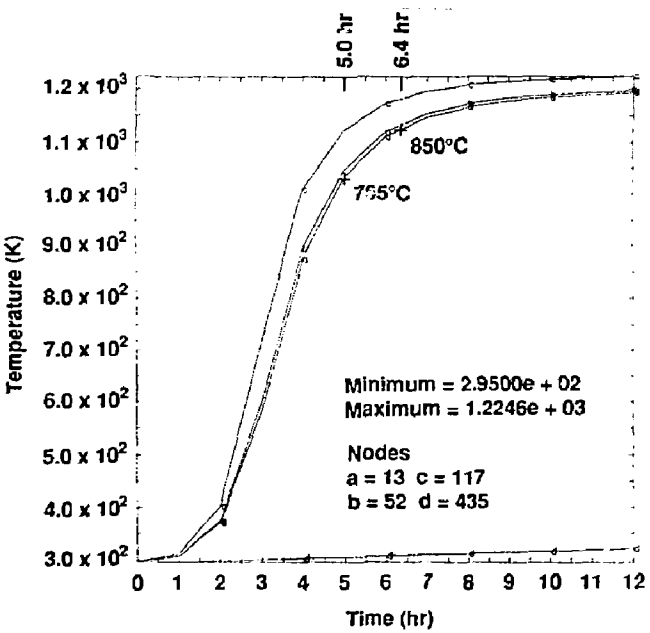

Figure 17. Temperature history of an Al_2O_3 container (half scale, 3-in.-thick wall) with heating Profile 3.

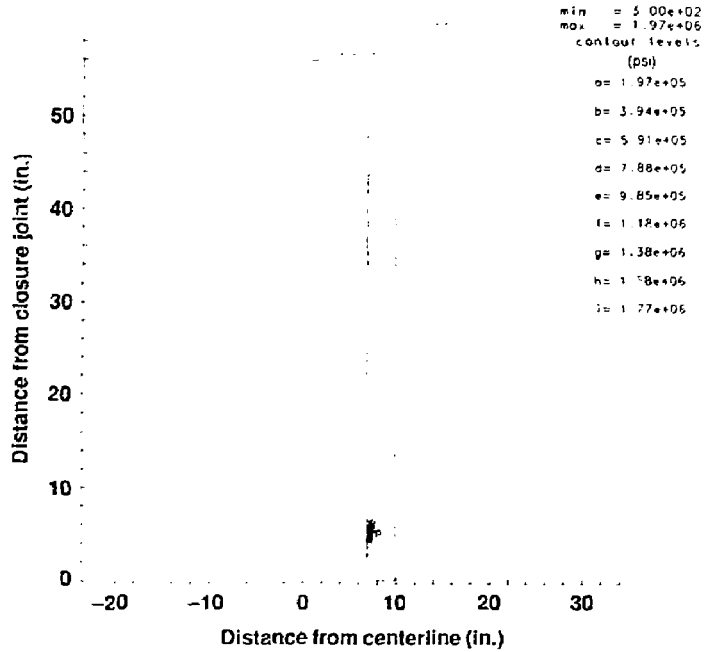

Figure 18. Thermal stress associated with heating Profile 1 (half scale, 3-in.-thick wall).

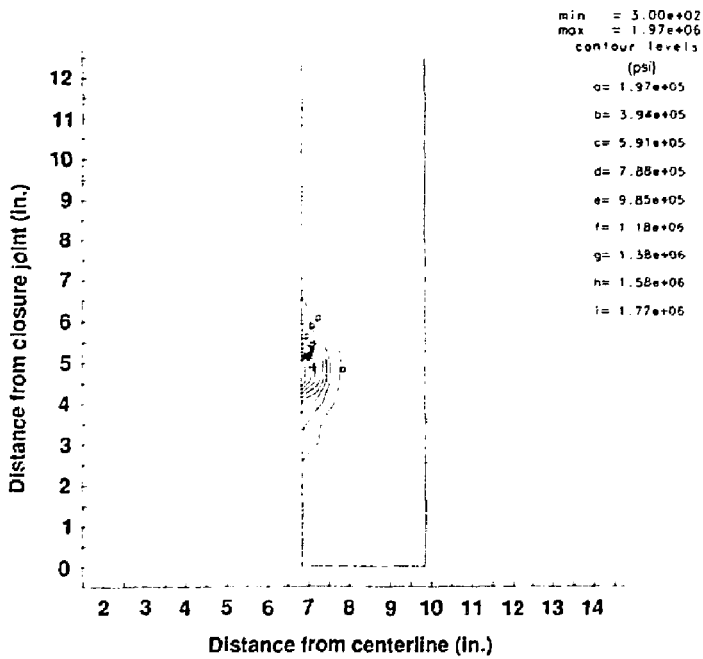

Figure 19. Thermal stress close-up view for heating Profile 1.

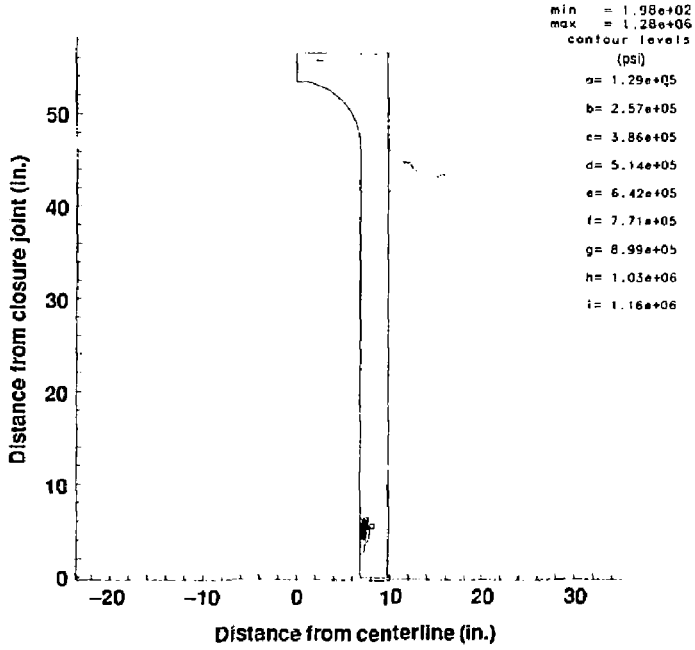

Figure 20. Thermal stress associated with heating Profile 2 (half scale, 3-in.-thick wall).

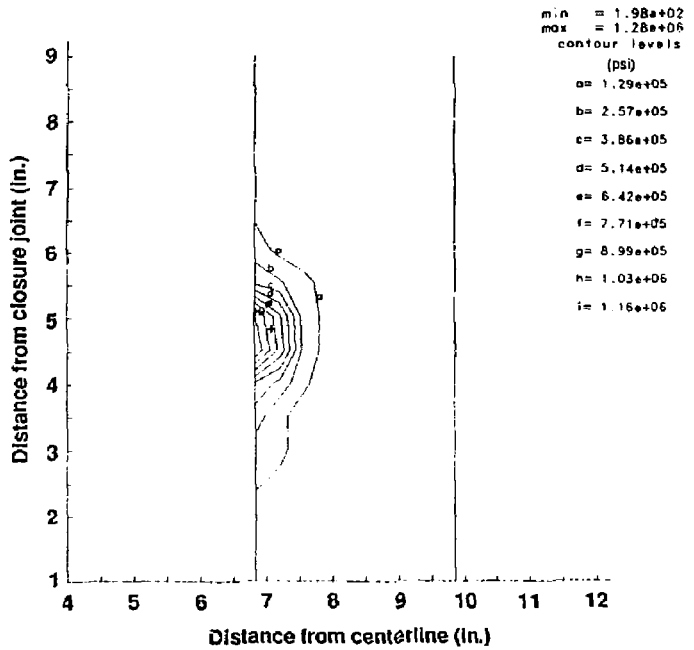

Figure 21. Thermal stress close-up view for heating Profile 2.

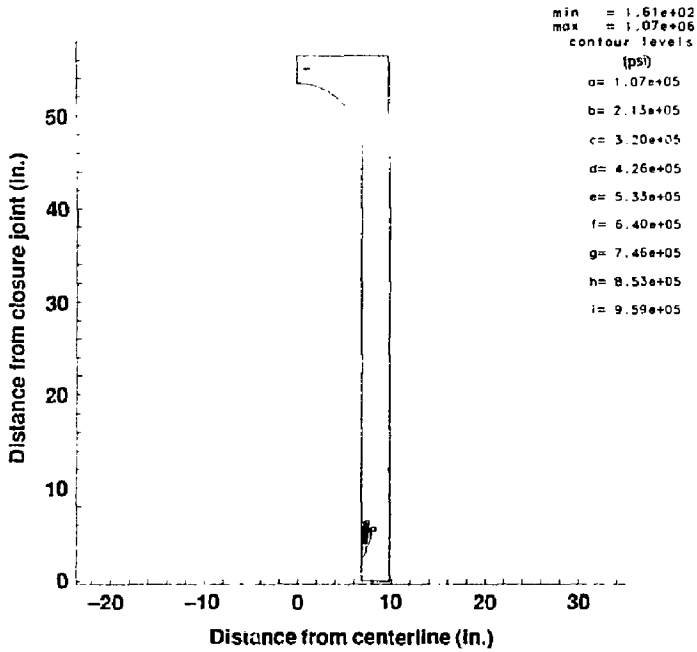

Figure 22. Thermal stress associated with heating Profile 3 (half scale, 3-in.-thick wall).

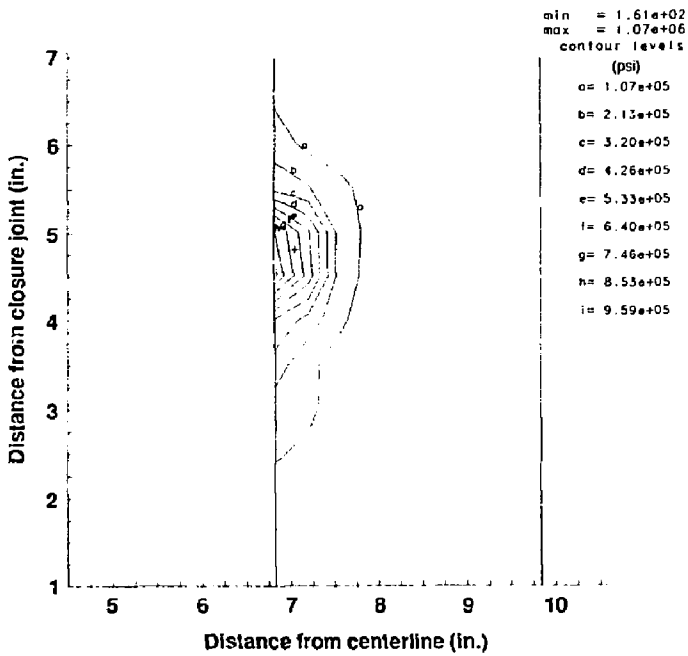

Figure 23. Thermal stress close-up view for heating Profile 3.